

## Article

# Water Yield Responses to Gradual Changes in Forest Structure and Species Composition in a Subboreal Watershed in Northeastern China

Zhengxiang Yu <sup>1</sup>, Ge Sun <sup>2</sup>, Tiji Cai <sup>1,\*</sup>, Dennis W. Hallema <sup>2,3</sup> and Liangliang Duan <sup>1</sup> 

<sup>1</sup> Department of Forestry, School of Forestry, Northeast Forestry University, Harbin 150040, China; nefu\_yzx@163.com (Z.Y.); Liangliang.duan@nefu.edu.cn (L.D.)

<sup>2</sup> Eastern Forest Environmental Threat Assessment Center, U.S. Department of Agriculture Forest Service Southern Research Station, Research Triangle Park, NC 27709, USA; ge.sun@usda.gov

<sup>3</sup> Oak Ridge Institute for Science and Education, U.S. Department of Energy, Oak Ridge, TN 37830, USA; dwhallem@ncsu.edu

\* Correspondence: tiji.cai@nefu.edu.cn; Tel.: +86-045182191821

Received: 16 January 2019; Accepted: 26 February 2019; Published: 27 February 2019



**Abstract:** Relationships between forest cover and streamflow have been studied worldwide, but only a few studies have examined how gradual changes in forest structure and species composition due to logging and climate change affect watershed water yield ( $Q$ ) and flow regimes. In this study, we analyzed long-term (45 years) hydrologic, climate and forest dynamics data from the subboreal Tahe watershed in northeastern China. Our purpose was to evaluate the effects of forest logging and regeneration on changes in forest biomass and species and to quantify the subsequent impact on mean annual streamflow and flow regime under a changing climate. The study watershed was dominated by old-growth larch (*Larix gmelinii* Rupr.) during the 1970s, but gradually transformed into young deciduous larch mixed with deciduous broad-leaved birch (*Betula platyphylla* Sukaczew) during the 2010s. During the same period, the watershed experienced climate change with a significant increase in air temperature of  $0.028\text{ }^{\circ}\text{C}/\text{year}$ . We applied eight sensitivity-based techniques to separate the effects of climate change on water yield from those due to forest changes. We used flow duration curves (FDCs) to characterize flow regimes by dividing the study into four key periods based on the proportional change of larch and birch trees. We found that the mean annual streamflow decreased by 10 mm ( $-16\text{ mm}$  attributed to forest change and  $+6\text{ mm}$  to climate change) between the 1984–1994 period and the 2006–2016 period when the proportion of birch increased by 20% with a similar total forest volume in the later period. The mean annual streamflow increased from 216 mm to 270 mm ( $+35.5\text{ mm}$  due to forest change vs  $+17.7\text{ mm}$  due to climate change) when forest volume decreased by 18.7% ( $17\text{ m}^3/\text{ha}$ ) between the 1970s and 1984–1994. Water yield changed only slightly (3.5 mm) when forest volume increased by 8.7% ( $6\text{ m}^3/\text{ha}$ ) from 2000 to 2011. In addition, the magnitude of high flow and low flow increased following deforestation and a shift in species composition from a period (1984–1994) with 70% larch with 30% birch to a later period (2006–2016) with 50% larch with 50% birch. Both high flow and low flow decreased coinciding with a reforestation period (2006–2016). Our results highlight complex interactions among climate, forest structure, total biomass, and plant diversity (trees species composition) in influencing watershed hydrology. Further study is needed to examine the effects of ecohydrological processes such as evapotranspiration in larch and birch forests on hydrologic changes across multiple scales.

**Keywords:** climate change; forest structure change; species composition shift; forest hydrology; flow regime; water yield

## 1. Introduction

Understanding the relationship between forests and watershed hydrology or water supply is critical for the sustainable management of headwaters worldwide. Most forest hydrological research efforts have focused on the hydrologic effects of forest cover changes such as logging, reforestation, or afforestation. Review studies on this topic showed that deforestation increases annual water yield while reforestation decreases it [1–3]. However, few studies have examined the effects of combined gradual changes in forest structure and species composition shift on watershed hydrology. An early study published by Swank and Miner [4], Swank and Douglass [5] found that the conversion of broadleaf forests to evergreen coniferous forests reduced water yield by more than 30% in the southern Appalachians in the U.S. A series of related studies also suggested species change could have appreciable impacts on streamflow in small watersheds. For instance, Serengil et al. [6] showed that converting mixed deciduous forests to pine forests caused minor effects on high flows while the high flow returns periods and low flow decreased with the conversion of mixed deciduous forest to pine. Brantley et al. [7] showed that a shift from evergreen hemlock (*Tsuga canadensis* (L.) Carr.) to deciduous species can potentially result in a permanent reduction in winter evapotranspiration (ET) and an increase in winter streamflow. Caldwell et al. [8] showed that a shift in dominance from xerophytic oak and hickory species to several mesophytic species decreased water yield by as much as 18% in a given year. Elliott et al. [9] demonstrated that the decline in streamflow could be explained by the shift in major forest species from predominantly *Quercus* and *Carya* to predominantly *Liriodendron* and *Acer*. However, the U.S. studies are in contrast with results for Japan, where broad leaved forests did not use more water than coniferous forests [10–12]. A study by Sun et al. [13] in southern China suggested that natural regeneration in a watershed dominated by Chinese fir (*Cunninghamia Lancilanta*) plantations might have caused a decrease in streamflow. As far as we know, no studies have examined the effects of converting deciduous conifer forests to mixed coniferous and broad-leaved forests in a subboreal climate in Northeast China.

Changes in forest structure and species composition affect the total water balance of a watershed by changing the total amount of ET, equal to the sum of canopy evaporation, evaporation from the forest floor, and tree transpiration [8,14,15]. Plant water use and transpiration rates at the leaf, tree, and stand levels differ greatly among species [16,17] due to xylem anatomy, sapwood area, and leaf biomass [18]. Species with a ring-porous xylem anatomy, diffuse-porous xylem, semi-ring porous xylem, and tracheid xylem anatomies have different physiological characteristics in transpiring water for a given stem diameter [8,19]. As a result, changes in forest structure and species composition could impact ET and water yield from forested watersheds. Hydrological changes due to vegetation change have potential consequences for important hydrologic services, including water supply for human water consumption, agriculture, and industry, and for downstream biodiversity and aquatic ecosystem health [20].

In many large watersheds, climate change and forest dynamics are two major drivers of hydrologic change [21,22]. To quantify the true impact of forests on streamflow, the impacts of climate change must be distinguished from one another, which can be done with statistical or process-based modeling methods [23]. Examples of these methods are hydrologic trend analysis [24], time trend method [25], double mass curves [26], modified double mass curves [22], water balance [27], and sensitivity-based methods [28,29].

The Da Hinggan Mountains in subboreal Northeast China is known for its importance in timber production in China. Forest resources declined dramatically in the 1960s–1990s due to heavy logging, from a forest stock of 460 million cubic meters in the 1960s to 0.18 million in the 2010s. Reforestation programs began in the 2000s after logging activities subsided. In addition, the Da Hinggan Mountains form the headwaters of the Heilongjiang River and the Nenjiang River. Sustainable water supply is one of the critical ecological challenges for the regions downstream. The downstream Songnen-Sanjiang Plain is now a grain production area of major national importance [30], and contains the largest wetland in Northeast China [31]. In order to reduce

the risk of water shortages for agriculture and wetlands due to climate change [32], there is an urgent need to better understand the impacts of forest changes on water yield.

The goal of this study was to examine how historic gradual deforestation and reforestation activities affected streamflow and water supply in a region that has seen gradual forest changes over the past four decades. As a case study, we selected one large watershed (6581 km<sup>2</sup>) with long-term (40 years) data for hydrometeorology, land cover and forest resource inventory. The specific key objectives were: (1) to analyze the changes in climate, streamflow and forest structure over time; (2) to quantify the individual impact of climate variation and forest structure change on streamflow; and (3) to determine how forest composition altered the flow regimes.

## 2. Study Watershed and Databases

### 2.1. Study Watershed

The Tahe watershed (124°23′54″–124°49′02″ N, 51°27′03″–51°39′22″ E) is located on the northern slopes of Da Hinggan Mountains in Heilongjiang Province, northeastern China (Figure 1a). The watershed represents a first-order tributary of the Huma River, which drains to the Heilongjiang River, the world's tenth longest river forming the border between the Russian Far East and northeastern China [33]. The watershed covers an area of 6581 km<sup>2</sup> and the main channel length is 148 km. The topography is characterized by moderate hills divided by a broad valley [34], and the elevation ranges from 340 m to 1309 m above sea level. Three quarters of the watershed area has an elevation between 573–834 m and a mean slope of ~20% (Figure 1b). The forests are dominated by Larch (*Larix gmelinii*), Mongolian pines (*Pinus sylvestris* var. *mongolica*) and Picea (*Picea koraiensis* Nakai), and broadleaf species, such as Birch (*Betula platyphylla*), Poplar (*Populus davidiana* Dode). The climate is classified as a boreal-temperate continental monsoon. The average annual precipitation is 505 mm, of which 75% falls between June to September and 10% of precipitation is snow. Elevated temperatures often coincide with high precipitation volume. The mean annual air temperature is −2.2 °C, with an average high of 25.2 °C in July and an average low of −32.2 °C in January (Figure 2).

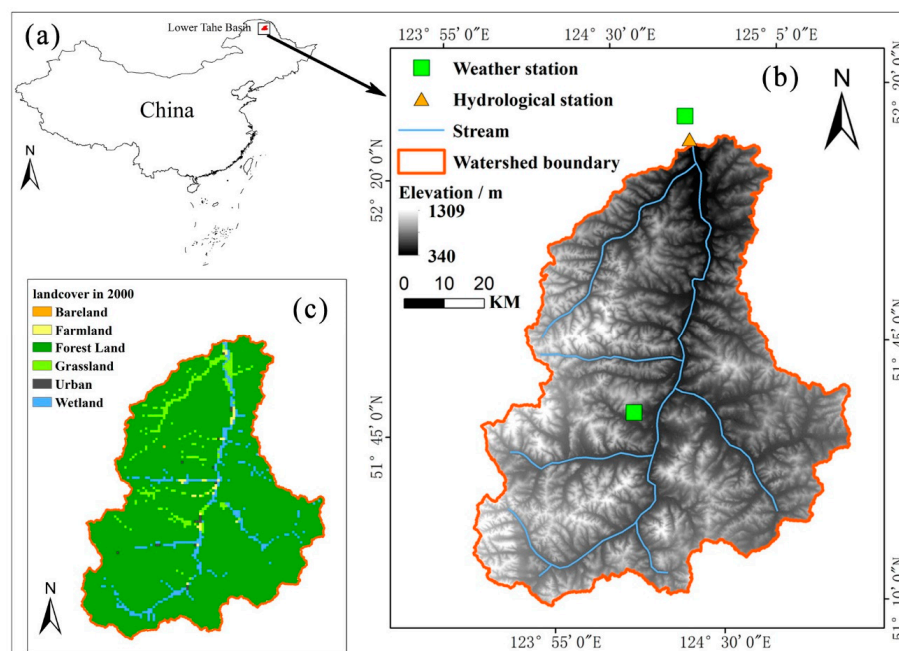


**Figure 1.** (a) Location of the study watershed in China, (b) Two meteorological stations, hydrological station, and Digital Elevation Model (DEM) of the Tahe watershed, and (c) Land cover in 2000.

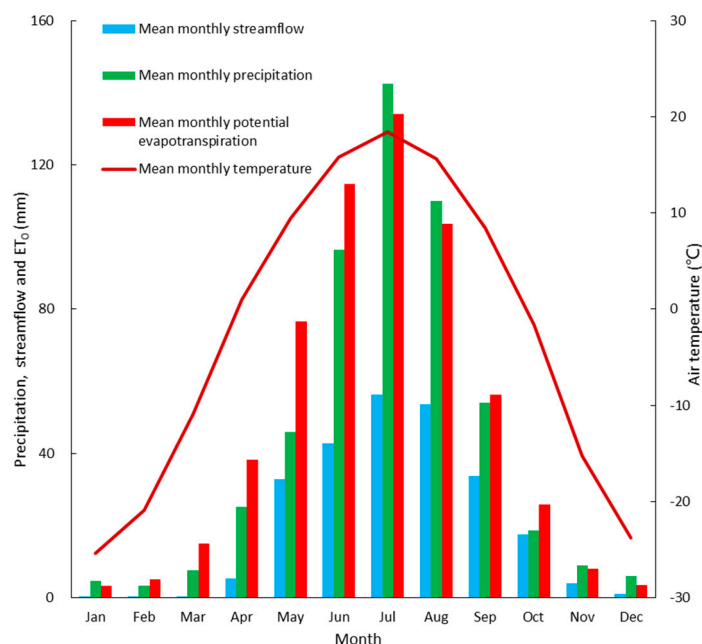


**Figure 2.** Mean monthly streamflow, precipitation, potential evapotranspiration ( $ET_0$ ) and air temperature in the Tahe watershed from 1972 to 2016.

## 2.2. Climate, Hydrology, and Landuse

We followed the protocol of “Observation Methodology for Long-term Forest Ecosystem Research” of the National Standards of the People’s Republic of China (GB/T 33027–2016) to acquire daily streamflow for the Xinlin hydrologic station from 1973 to 2016 (data missing in 1983). The daily mean ( $T_{mean}$ ), maximum ( $T_{max}$ ), minimum ( $T_{min}$ ) air temperatures, daily precipitation ( $P$ ) and daily mean wind speed were obtained from Xinlin climate station (Climate ID: 50349) and Tahe climate station (Climate Station ID: 50246) (Figure 1b) and were provided by the China Meteorological Administration (CMA) (<http://cdc.cma.gov.cn>).

The Land Use / Land Cover Change (LULCC) Data Set [35] that was generated from remote sensing imagery was used to determine the land use changes for 1990, 2000, and 2010. This dataset was provided by the Data Center for Resources and Environmental Sciences, Chinese Academy of Sciences (<http://www.resdc.cn>). The land cover type was dominated by forest lands, which changed only slightly from 90.9% to 90.3% during the past three decades. Consequently, land cover in the Tahe watershed was fairly stable over time (Table 1).

**Table 1.** Land use in the Tahe watershed in 1990, 2000 and 2010.

Time	1990		2000		2010	
	Area (km <sup>2</sup> )	Percentage (%)	Area (km <sup>2</sup> )	Percentage (%)	Area (km <sup>2</sup> )	Percentage (%)
Forest land	5997	90.9	5984	90.7	5957	90.3
Grass land	245	3.71	235	3.6	262	4.0
Urban and builtup land	23	0.35	19	0.3	19	0.3
Farmland	24	0.36	36	0.6	36	0.6
Fen wetland	304	4.61	319	4.8	319	4.8
Water body	4	0.06	4	0.1	4	0.1

## 2.3. Forest Composition Shift

Forest species composition and volume data were obtained from 1986, 1994, 2007 and 2013 forest resource inventory datasets maintained by the Xinlin Forestry Bureau. The forest composition was almost 100% larch-dominated prior to the 1970s [33], and the volume of the forest was over 90 m<sup>3</sup>/ha before widespread deforestation in the 1980s. The historical deforestation consisted of clear-cutting

mature stands, and selective-cutting middle-aged stands. At the same time, larch plantations and birch secondary growth started to appear on the clear-cut land (Figures 3 and 4). During the study period 1986–2007 the forests experienced both harvesting and restoration, the deciduous coniferous larch forests gradually decreased, and the broadleaf deciduous forest (mostly birch) gradually increased. After 2007, forests mainly experienced restoration due to the Natural Forest Protection Project; forest species proportion minor changed, and forest volume gradually increased.

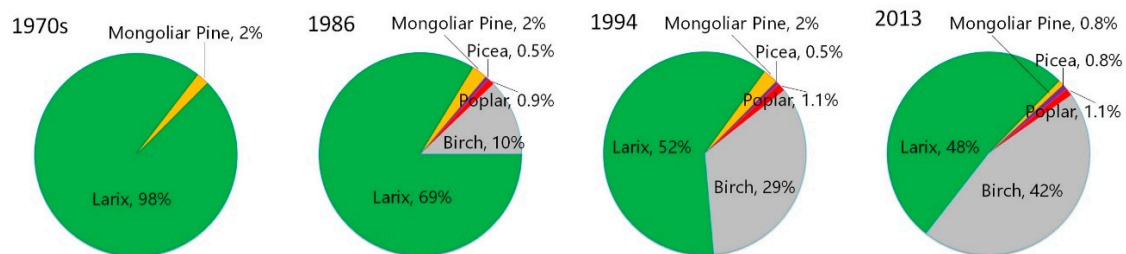


Figure 3. Area of tree species in 1970, 1986, 1994 and 2013.

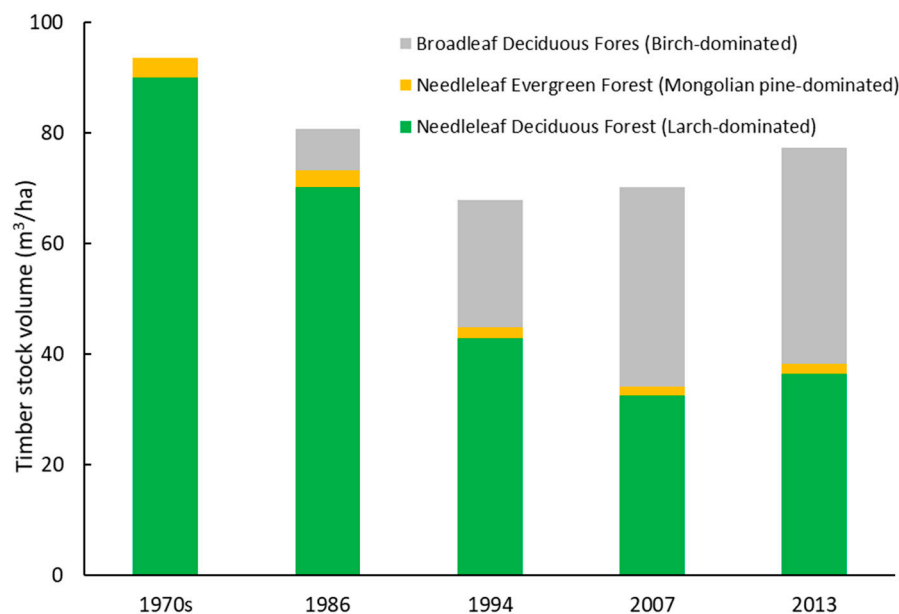


Figure 4. Timber stock volume per hectare of the three forest types in the 1970s, 1986, 1994, 2007 and 2013.

### 3. Hydrologic Analysis Methods

Based on the 5-year historical forest resource inventory data, we first divided the study period into four periods that had unique forest species compositions. Then, the changes in mean annual streamflow and flow regime characterization were analysed in the four periods. We assumed that climate variability and forest change were the two major factors that could explain streamflow change. To quantify the sole effects of forest changes on streamflow, the impact of climate variations needs to be separated from the total observed hydrologic changes: (1) Flow duration curves (FDCs) were used for each period to characterize the long-term changes in streamflow regimes, and the paired year approach was adopted to eliminate the effect of climate variations and understand the impact of forest changes on flow regime characterization. (2) The climate elasticity models were used to calculate the portion of the mean annual streamflow that was affected by climate variations, and the other portion in the total change of mean annual streamflow was due to forest changes.



### 3.1. Four Periods for Hydrologic Change Analysis

We subdivided the entire study period into four periods based on the proportional change of larch and birch trees.

Period 1: 1972–1982, larch accounted for almost 100% of the forest area;

Period 2: 1984–1994, 70% of larch with 30% of birch;

Period 3: 1995–2005, 60% of larch with 40% of birch;

Period 4: 2006–2016, 50% of larch with 50% of birch.

Tree species other than larch and birch covered only a minor portion of the watershed and were not considered in defining these periods. Based on the historic Forest Resource Inventory datasets (Figure 4), a linear regression was used to interpolate the forest stock volume for any year during the study periods.

In order to make the results more representative, three sets of comparisons in different periods were performed to explore the annual streamflow change due to forest structure change and species composition shift:

First, the effect of deforestation on streamflow was obtained by comparing Period 1 and Period 2. During Period 2, the total stock volume of the forest decreased by 18.7%, which included the volume of larch that decreased by 30 m<sup>3</sup>/ha and the volume of birch that increased by 13 m<sup>3</sup>/ha, while the forest species shifted from 100% larch to 70% larch with 30% birch. The proportion of birch increased due to the natural forest succession as young forests presumably use less water, and the change in streamflow was mainly caused by deforestation.

Second, streamflow change between Period 2 and Period 4 was considered to be the effects of species composition shift. The total forest stock volume was similar between the two periods (around 75 m<sup>3</sup>/ha). Meanwhile, the forest species shifted from 70% larch with 30% birch to 50% larch with 50% birch, and the stock volume of larch decreased by 41.2% and the stock volume of birch increased by 186.6%.

Third, Period 3 was compared with Period 4 to evaluate the impact of reforestation on streamflow. The total stock volume of forest increased from 68 m<sup>3</sup>/ha to 75 m<sup>3</sup>/ha, which included a minor decrease of 3 m<sup>3</sup>/ha in the larch stock volume; the volume of birch increased by 10 m<sup>3</sup>/ha, while only 10% larch shifted to birch.

### 3.2. Flow Regime Characterization

Information on high and low flows is essential to ensure aquatic biodiversity and functional integrity of river ecosystems [36]. Flow Duration Curves (FDCs) show the percentage of time during which a given magnitude of streamflow is exceeded, and this characteristic makes it a useful indicator of hydrologic change [3]. The percentage represents the probability of exceedance  $p$  of a given discharge,  $Q$ , where  $p$  is defined by  $p = 1 - P\{Q \leq q\}$  [37,38]. Similarly, the precipitation duration curves (PDCs) characterize daily precipitation patterns.

We used FDCs to define high and low flow regimes. High flows are defined as the flows that equal to or are greater than  $Q_5$  ( $Q_5$ : flow exceeded for 5% of the time in a given year) [39,40]. During winters, the rivers are covered by ice, and the runoff was extremely small. Low flows refer to the flows that are equal to or less than  $Q_{70}$  ( $Q_{70}$ : flows exceeded for 70% of the time in a given year) [41].

In order to eliminate the effect of climate variation and understand the impact of forest change on flow regimes, the paired year approach developed by Zhang and Wei [42] was adopted in this study. The paired year approach used Kendall's tau and Spearman correlation analyses to test the correlations between hydrological variables (high flow magnitude and low flow magnitude) and climatic variables (annual precipitation, wind speed, mean annual temperature, maximum temperature, and minimum temperature). The significant climatic variables were identified when the results from two methods both showed significant correlations. Each paired years from different periods were selected according to the most relevant climate variables.

### 3.3. Climate Elasticity of Mean Annual Streamflow

Changes in observed mean annual streamflow ( $\Delta Q^{tot}$ ) were attributed to climate variability ( $\Delta Q^C$ ) and forest change ( $\Delta Q^H$ ) as follows [43,44].

$$\Delta Q^{tot} = \Delta Q^C + \Delta Q^H \quad (1)$$

We applied the widely used climate elasticity model developed by Shaake [45] to evaluate the sensitivity of streamflow to climate change and separate streamflow impacts caused by climate change from human activities:

$$\varepsilon = \frac{dQ/Q}{dX/X} \quad (2)$$

The climate elasticity of streamflow ( $\varepsilon$ ) is defined by the proportional change in streamflow ( $Q$ ) divided by the proportional change in a climate variable  $X$ , such as  $P$ , temperature, or potential evapotranspiration ( $ET_0$ ).

$ET_0$  is preferred to temperature because  $ET_0$  better reflects the direct effects of climate change on streamflow [29,46]. The approach used to calculate  $ET_0$  is provided in Supplement S1. According to Sankarasubramanian et al. [47], Zheng et al. [29],  $\Delta Q^C$  is estimated from  $\Delta P$ ,  $\Delta ET_0$  (changes in precipitation  $P$  and  $ET_0$  between the different phases) using the following equation:

$$\Delta Q^C = (\varepsilon_P \Delta P / \bar{P} + \varepsilon_{ET_0} \Delta ET_0 / \overline{ET_0}) \bar{Q}, \quad \text{and } \varepsilon_P + \varepsilon_{E_0} = 1 \quad (3)$$

where  $\varepsilon_P$  and  $\varepsilon_{ET_0}$  are the  $P$  and  $ET_0$  elasticity coefficients, respectively. Over-bars represent the mean over the combined baseline and post treatment periods. Mean annual streamflow changes between each 'post treatment' period and the baseline period (Period 1) were examined using sensitivity-based method. To reduce uncertainty for different analytic methods, we used multiplication techniques in this study including non-parametric and Budyko framework-based approaches.

#### 3.3.1. Nonparametric Estimator of $\varepsilon_P$

Sankarasubramanian et al. [47] proposed a nonparametric approach to estimate the climate elasticity directly from observed hydrologic data. This method has been used in the United States [47], Australia [28,48] and China [29], and Zheng et al. [29] rewrote the equation as follows:

$$\varepsilon_P = \text{median} \left[ \frac{(Q_i - \bar{Q}) / \bar{Q}}{(P_i - \bar{P}) / \bar{P}} \right] \quad (4)$$

In addition, an alternative nonparametric of climate elasticity ( $\varepsilon_P$ ,  $\varepsilon_{E_0}$ ) is a multiple regression equation (Equation (5)) and can be estimated using the least squares estimator [29,49].

$$\varepsilon = \frac{\bar{X}}{\bar{Q}} \cdot \frac{\sum (X_i - \bar{X})(Q_i - \bar{Q})}{\sum (X_i - \bar{X})^2} = \rho_{X,Q} \cdot C_Q / C_X \quad (5)$$

where  $\rho_{X,Q}$  is the correlation coefficient of  $X$  and  $Q$ , and  $C_X$  and  $C_Q$  are coefficients of variation of  $X$  and  $Q$ , respectively.

#### 3.3.2. Budyko framework for Estimating $\varepsilon_P$

According to the Budyko [50], mean actual evapotranspiration ( $\bar{E}$ ) is a function of aridity index ( $AI = \overline{ET_0} / \bar{P}$ ).

$$\bar{E} = \bar{P} F(AI) \quad (6)$$

The precipitation elasticity of streamflow can be expressed using the following equation.

$$\varepsilon_P = 1 + \frac{AIF'(AI)}{1 - F(AI)} \quad (7)$$

According to the Equation (7),  $\varepsilon_P$  can be estimated for a given AI, once the form of  $F(AI)$  is given, ( $F'(AI)$  is the derivative of  $F(AI)$ ). We calculated six forms of  $F(AI)$  based on the Budyko hypothesis (Table 2).

**Table 2.** A summary of methods for estimating annual actual evapotranspiration based on the Budyko Hypothesis.

Expression Form	$F(AI)$
Schreiber [51]	$F(x) = e^{-AI}$
Ol'Dekop [52]	$F(x) = AI \tanh(1/AI)$
Budyko [50]	$F(x) = AI \tanh(1/AI) (1 - e^{-AI})^{0.5}$
Pike [53]	$F(x) = 1/\sqrt{1 + AI^{-2}}$
Fu [54]	$F(x) = 1 + AI - (1 + AI^\alpha)^{1/\alpha}, \alpha = 2.5$
Foster [37], Sun et al. [34]	$F(x) = (1 + wAI)/(1 + wAI + 1/AI), w = 2$

## 4. Results

### 4.1. Changes in Climate and Streamflow

The mean annual temperature and mean maximum temperature followed a significant positive trend ( $p < 0.01$ ) during the entire study period (1972–2016), with an increase of  $0.028^\circ\text{C}/\text{year}$  and  $0.043^\circ\text{C}/\text{year}$ , respectively. The  $ET_0$  also followed a significant positive trend ( $1.4 \text{ mm}/\text{year}$ ,  $p < 0.01$ , Kendall tau). However, there were no statistically significant linear trends across all years in annual streamflow, mean minimum temperature, precipitation, or runoff ratio (Table 3).

**Table 3.** Hydrological and climatic changes for study period.

Variable	Q/mm	P/mm	Runoff Ratio	ET/mm	$ET_0/\text{mm}$	T/ $^\circ\text{C}$	Tmax/ $^\circ\text{C}$	Tmin/ $^\circ\text{C}$
Mean	247	490	0.46	243	562	−2.05	5.12	−8.22
Slope	0.7	0.9	0.07%	0.1	<b><u>1.4</u><sup>1</sup></b>	<b><u>0.028</u></b>	<b><u>0.043</u></b>	0.018

Note: Q = annual streamflow; P = annual precipitation; ET = actual evapotranspiration calculated as P-Q;  $ET_0$  = potential evapotranspiration calculated by the Hamon method; T = mean annual air temperature. Bold underlined values indicate the trends with statistical significance of  $p < 0.01$ . <sup>1</sup> Bold values indicate the trends with statistical significance of  $p < 0.05$ .

Compared with Period 1, the mean annual precipitation in Period 2 increased by 28 mm (5%) with a 21 mm increase in mean annual  $ET_0$  (Figure 5). The annual streamflow increased by 53 mm (24%) and the runoff coefficients increased by 17.8%. These changes coincide with a period of massive deforestation of larch forests. Compared with Period 2, Period 4 had 17 mm higher mean annual precipitation with a 19 mm increase in mean annual  $ET_0$ . During this period, with species composition shift, mean annual streamflow and Q/P ratios decreased by 3% and 8%, respectively. Forest harvesting slowed down during Period 4 and the forests partially recovered. Compared with Period 3, mean annual precipitation increased by 27 mm in Period 4 and the mean annual  $ET_0$  increased by 11 mm. The mean annual streamflow increased by 7% and with negligible change in Q/P ratios. In order to single out the impacts of forest changes on streamflow, climate effects of the increase in  $ET_0$  and the variability of precipitation should be eliminated as presented in the following sections.



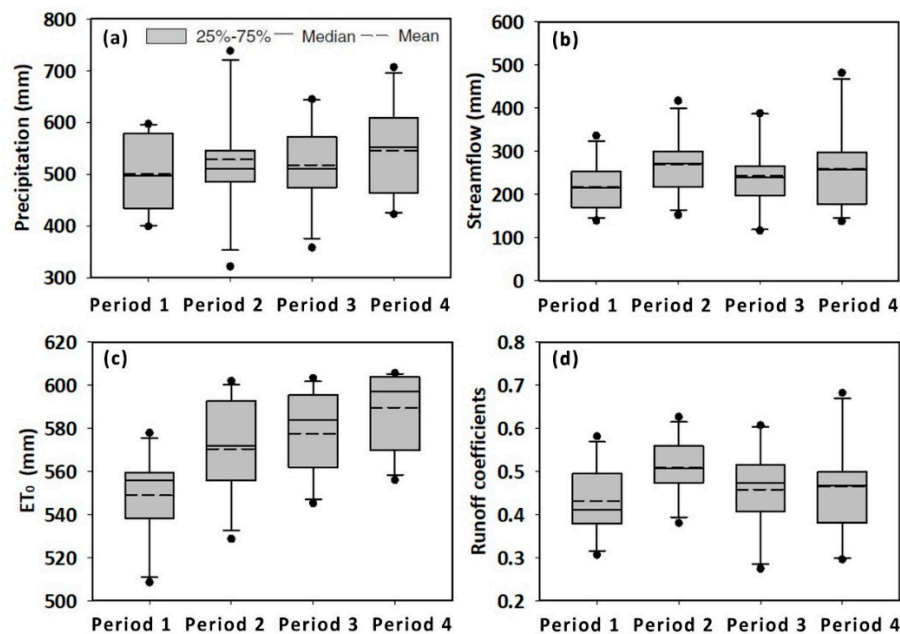


**Figure 5.** (a) The precipitation in four periods; (b) The streamflow in four periods; (c) The  $ET_0$  in four periods; (d) The runoff coefficients in four periods. Period 1 = 1972–1982, Period 2 = 1984–1994, Period 3 = 1995–2005, Period 4 = 2006–2016.

#### 4.2. Impacts of Forest Change on Annual Streamflow

The eight methods provided comparable results (Table S1 and Figure S1). Thus, the means were used to separate the respective influences of climate and forest structure and species composition on annual streamflow.

Overall, the impact of forest change ( $\Delta\overline{Q_F}$ ) on annual streamflow declined gradually with forest recovery (Table 4). First, the mean annual streamflow increased by 35.5 mm due to deforestation during Period 2, when forest change accounted for 65.7% of total change. Second, the forest species composition between Period 2 and Period 4 reduced the mean annual streamflow of 16 mm. Third, the impact of reforestation on annual streamflow between Period 3 and Period 4 decreased mean annual streamflow by 3.2 mm. In addition, climate changes in  $P$  and  $ET_0$  caused an increase in mean annual streamflow up to 11.1% during the highest precipitation period (Period 4). However, the climate contribution to this change was minor (1.6%) during the period with the lowest precipitation (Period 3).

**Table 4.** Attribution of forest composition change and climate variability to mean annual streamflow change.

Period	$\Delta P$ (mm)	$\Delta \overline{PET}$ (mm)	$\Delta \overline{Q_{tot}}$ (mm) and Relative Change	Forest $\Delta \overline{Q_F}$		Climate $\Delta \overline{Q_C}$	
				Absolute (mm) and Restively Change	Relative Contribution	Absolute (mm) and Relative Change	Relative Contribution
Period 1				Baseline Period			
Period 2	+27	+26	+54 (26%)	+35.5 (+16.4%)	65.7%	+17.7 (+8.1%)	34.3%
Period 3	+17	+36	+26 (11%)	+22.7 (+10.4%)	87.3%	+3.4 (+1.6%)	12.7%
Period 4	+45	+48	+44 (20%)	+19.5 (+9.0%)	44.3%	+24.0 (+11.1%)	55.7%

#### 4.3. Impacts of Forest Change on Flow Regimes

Daily high flows were strongly correlated with daily precipitation. The mean precipitation that exceeded 10% in the four periods was 17.7, 17.4, 15.4 and 19.4 mm (Figure 6c), and the mean magnitude of high flows was different (Figure 5a).

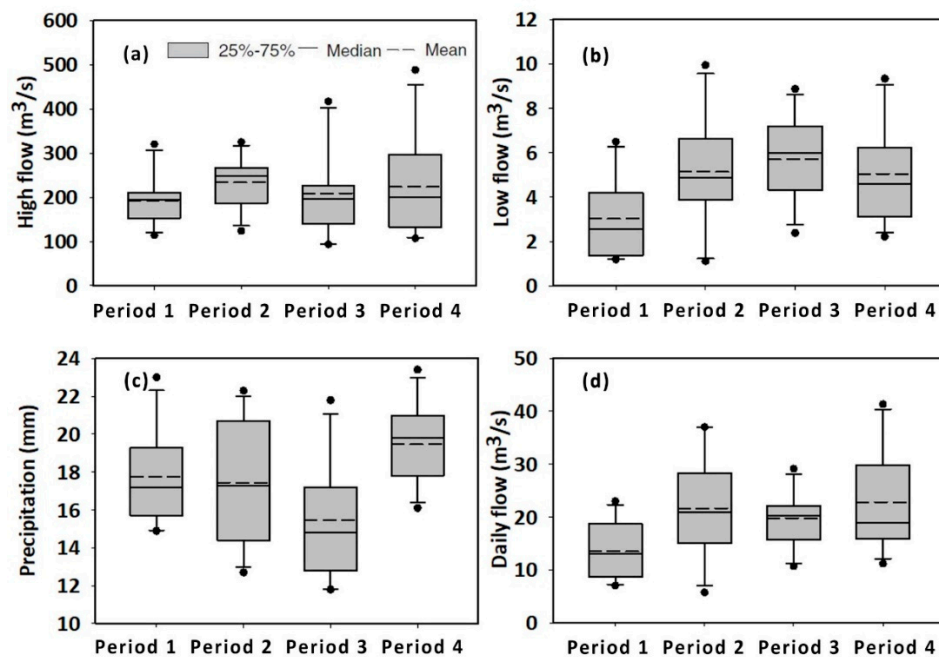


**Figure 6.** The magnitude of high flows (flow exceedance of 5%) in four periods (a); The magnitude of low flows (70% exceedance) in four periods (b); The precipitation exceeded at 10% (c); The daily flow exceeded 50% of the time in a given year (d). Period 1 = 1972–1982, Period 2 = 1984–1994, Period 3 = 1995–2005, Period 4 = 2006–2016.

Deforestation increased both high flows and low flows, but it decreased the high flow stability. The mean magnitude of high flow ( $193 \text{ m}^3/\text{s}$ ) in Period 1 was 20% lower than that in Period 2 ( $233 \text{ m}^3/\text{s}$ ), while the mean magnitude of low flow was increased from  $3 \text{ m}^3/\text{s}$  (Period 1) to  $5 \text{ m}^3/\text{s}$  (Period 2). On the contrary, the mean magnitude of high flow increased by only 7%, from Period 3 ( $208.7 \text{ m}^3/\text{s}$ ) to Period 4 ( $223.3 \text{ m}^3/\text{s}$ ), while the mean magnitude of low flow was similar between Period 3 ( $5.7 \text{ m}^3/\text{s}$ ) and Period 4 ( $5.1 \text{ m}^3/\text{s}$ ). The forest species composition change made high flow more unstable. Compared with Period 2, Period 4 was similar in the mean magnitude of high flow and lower in the 25%–75% interval of precipitation, but the 25%–75% interval of high flow exhibited great variability, i.e.,  $187 \text{ m}^3/\text{s}$ – $267 \text{ m}^3/\text{s}$  in Period 2 and  $133 \text{ m}^3/\text{s}$ – $297 \text{ m}^3/\text{s}$  in Period 4 (Figure 6a,c).

The detailed result of selecting the pairing year is described in the Supplementary Materials (Tables S2–S4). It appeared that the high flows for Period 1 were the lowest in all periods (Figure 7a–c), although the extreme precipitation in the period was higher (Figure S2). Compared with 2003 (Period 3) and 2009 (Period 4), 1990 (Period 2) had a lower high flow (Figure 7d,e). The 2012 high and low flows (Period 4) were lower than the 2000 (Period 3) high and low flows, respectively (Figure 7f). The low flow showed the same trend as high flow. As shown in Figure 8, the low flow of Period 1 was the lowest of all periods, and Period 2 experienced lower low flow than Period 3 and Period 4. In addition, the low flow in 1996 (Period 4) was 20% lower than that in 2010 (Period 3) with increasing forest volume. Overall, the forest species change from deciduous conifer forest to deciduous conifer broad-leaved mixed forest had a positive correlation with high flows and low flows, while the forest total volume was negatively correlated. (For details, see Supplementary Materials Figures S2–S7).

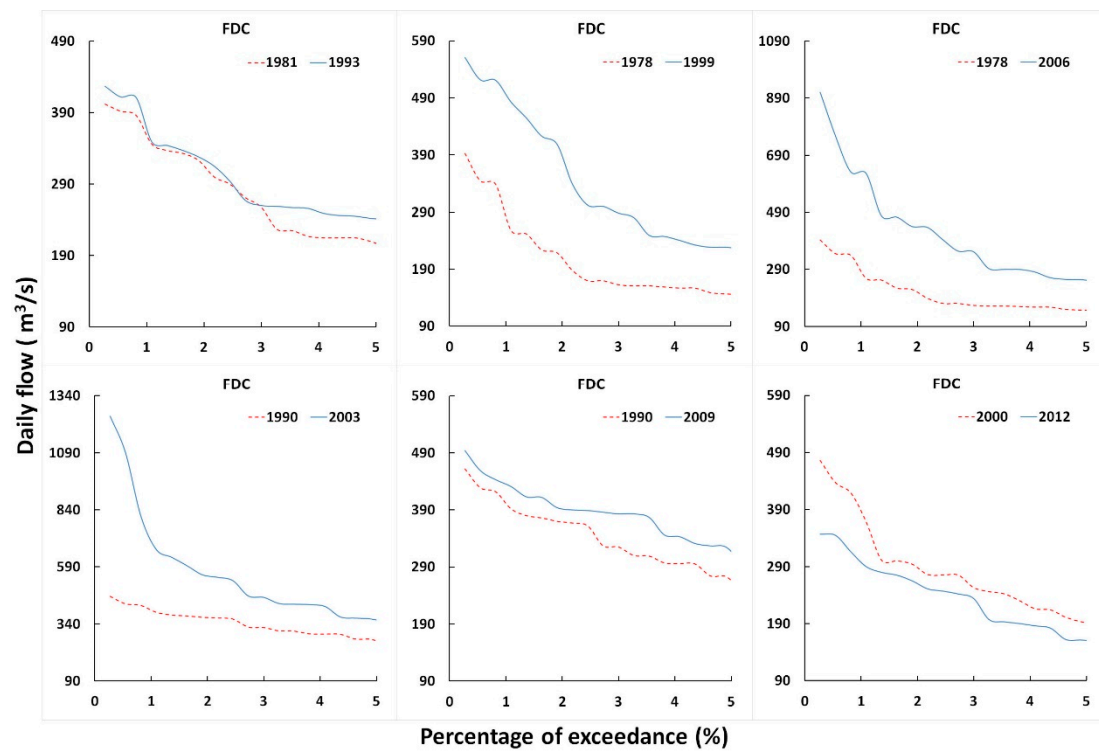


**Figure 7.** The selected paired years for high flow: 1981 vs 1993 (Period 1 vs Period 2) (a), 1978 vs 1999 (Period 1 vs Period 3) (b), 1978 vs 2006 (Period 1 vs Period 4) (c), 1990 vs 2003 (Period 2 birch vs Period 3 birch) (d), 1990 vs 2009 (Period 2 vs Period 4) (e), 2000 vs 2012 (Period 3 vs Period 4) (f).

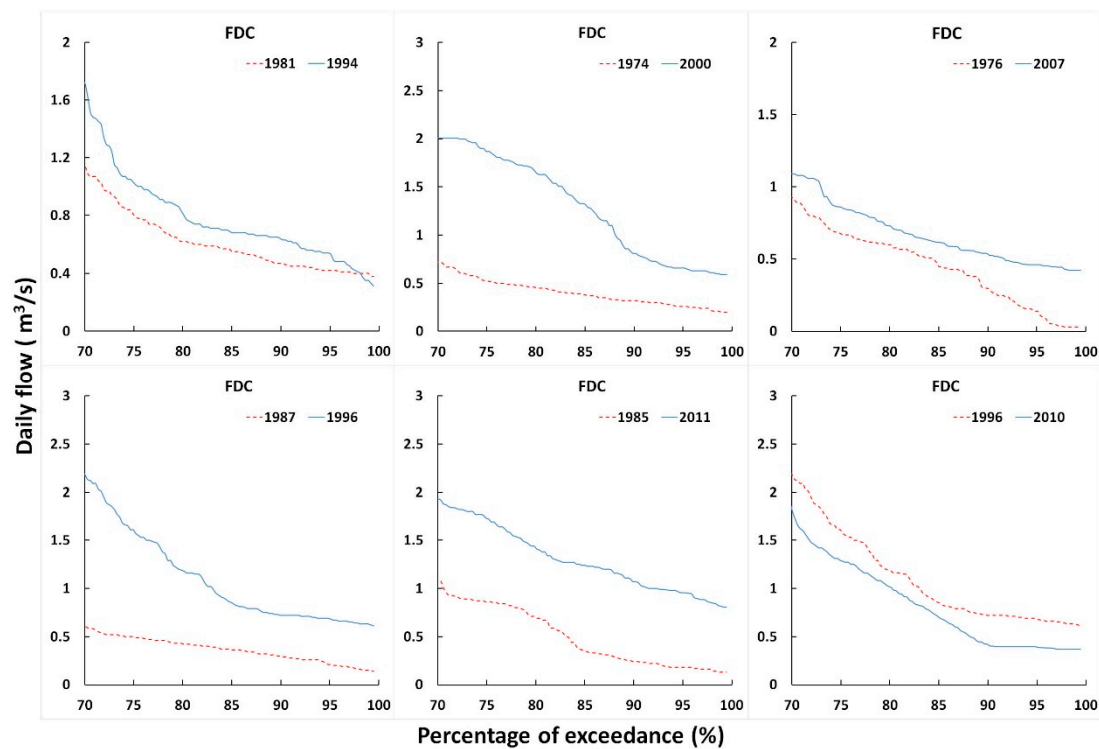


**Figure 8.** The selected paired years for low flow: 1981 vs 1994 (Period 1 vs Period 2) (a), 1974 vs 2000 (Period 1 vs Period 3) (b), 1976 vs 2007 (Period 1 vs Period 4) (c), 1987 vs 1996 (Period 2 vs Period 3) (d), 1985 vs 2011 (Period 2 vs Period 4) (e), 1996 vs 2010 (Period 3 vs Period 4) (f).

## 5. Discussion

### 5.1. The Effects of Forest Structure Change and Species Composition Shift on Annual Streamflow

Our results are consistent with a few studies on the impacts of deforestation and reforestation on annual streamflow in large watersheds (e.g., Li et al. [2]). Previous studies suggest the mechanisms are that deforestation decreases evapotranspiration [3,55] and reduces soil infiltration capacity due to soil erosion and compaction [40], while reforestation reverse these changes. Wang et al. [56] compared streamflow in 22 watersheds in our study region and concluded that both forest cover percentage and local climate, as modified by watershed elevations, controlled streamflow. It has long been established that plant biomass or leaf area has a major influence on ecosystem water use by the changes in ET [57]. Our study suggested that the gradual changes in the amount of forest cover altered tree water use patterns and consequently, streamflow.

A combination of changes in the physical processes (evaporation) and physiological processes (transpiration) may explain the detected streamflow change. First, the canopy interception of the secondary birch forest was lower than that of natural old-growth larch forest (about 8% of the total rainfall and 7.8% of total snowfall) [58–60]. In addition, litter interception may also be an important part of evaporation. The litter layer of the secondary growth birch forest would theoretically attenuate the negative effects of increased forest coverage on streamflow [33]. Second, the transpiration rates of birch trees are higher than those of larch trees. The main reason for the difference in transpiration between the two species was xylem anatomy type. The xylem anatomy type of larch consists of tracheids, and birch is diffuse-porous. The water use of diffuse-porous species is much higher than that of tracheid species for a given stem diameter [8,19,61]. Generally, the transpiration of conifer species is lower than that of broad-leaved species [53]. Due to the difference in climate zones, the case studies in the U.S. showed that coniferous forests use more water than broad-leaved forests, and the results were opposite in Japan [11,26]. In northern China, Zhang and Wang [62] showed that the transpiration of temperate broad-leaved forest is 1.72 times higher than the northern coniferous forest. Mu [63] showed that birch transpiration is almost twice that of larch when the air temperature is 20 °C. Unfortunately, there has been no detailed comparison study on sapflow of birch and larch trees in the Da Hinggan Mountain region. Further study is needed to quantify water use by individual trees and at the stand level to better understand the effects of species change on streamflow.

### 5.2. The Effects of Forest Structure Change and Species Composition Shift on Streamflow Regime

Several studies on deforestation impacts in rainfall-dominated regions [40,64,65] yielded conclusions similar to ours. For example, Kelly et al. [66] showed that forest structure change and species composition shift can enhance or lessen the effects of changes in precipitation patterns on high flow and low flow. Conversely, the conclusions for snowfall-dominated watersheds [67,68] were in contrast with our results.

We argue that the contrast might be caused by the drastic change in energy balances in boreal regions after a reduction in vegetation cover due to deforestation. It was reported that snowmelt within the lower elevation of a watershed often starts earlier in the spring season and occurs at a higher rate than at high elevations. The different snow melting patterns reduce the number of high flows [42]. In our study region, snowfall accounted for only approximately 10% of total precipitation. The annual streamflow hydrograph is characterized by high flows during spring, when snow melts, and summer, when rainfall peaks [39]. In spring, the snow was melting rapidly when the temperature increased suddenly, and most rainfall formed surface runoff with little infiltration because the soil was still frozen. In summer, with continuous precipitation, the decreased forest interception in deforestation and species composition shift [33], the reduction of the water-holding capacity of litter [69], added to reduced soil disturbance by erosion and compaction [40] increased the magnitude of high flow.

Regarding the impacts of forest change on low flow, studies on rain-dominated watersheds in China suggested that deforestation decreased the magnitude of low flows, while reforestation

increased it [24,40,70]. These studies claimed that soil infiltration capacity and water storage decreased (increased) when forests were degraded (restored). In contrast, our study showed that deforestation increased the magnitude of the low flow while reforestation decreased it. Our findings are more in line with other experimental studies outside China [65,71] that suggest that evapotranspiration is the main factor affecting the response of flow regimes to forest disturbances. We argue the soils may not be affected under the deforestation period in our study and thus change in ET is the main reason of observed hydrologic change. In addition, our watershed is located in a climate with cold winters and the frozen river had little flow during the winter period [72]. The low flows also occurred in the fall and spring. The low flow in the fall was affected by evapotranspiration, and the low flow in spring was affected by snow melt temperature. The high correlation between mean annual minimum temperature and low flow may further explain the temperature control on low flows (Table S2).

### 5.3. Implications and Uncertainty

Hydrology of headwater watersheds in Da Hinggan Mountains is not well understood due to the remoteness of the region in spite of the Heilongjiang River and the Nenjiang River. Songnen-Sanjiang Plain downstream of our study area being a major grain production region [30] with the largest wetland in northeastern China [31].

Our results indicated that reforestation decreased the mean annual streamflow by 16 mm and largely offset the climate impact (an increase in precipitation) on streamflow in the past decade. Forest water consumption increased gradually due to the increased biomass under the current forest management policies and rapid climate warming. If precipitation does not increase or become stable in the future, the reduction of annual water yield due to global warming forest regrowth is likely to cause stress of water demand for irrigation and wetlands in downstream [32,73]. In addition, our result indicated that the watersheds covered by primitive larch forests had a lower high flows and flood risk as compared with deciduous conifer broad-leaved mixed forests.

Our study suggests forest cover area (%) or timber stock volume may not be good indicators of forest hydrologic restoration success. Instead, forest biomass and species composition appear to best describe forest-water relations. Forest management that aims at reducing the frequency of floods [66] should consider forest structure, total biomass, and diversity (trees species composition).

Using multiple statistical methods to separate the hydrologic effects of forests from climate revealed several uncertainties. First, the six Budyko framework-based methods provide similar results. This is perhaps because those approaches use the same underlying concept to estimate the climate elasticity coefficients [28]. However, the results from the two non-parametric approaches had greater uncertainty. This was expected as all of these methods involve mathematically fitting. The temperature-based Hamon PET method was used to calculate  $ET_0$  due to the limited meteorological variables observed at the weather stations. Many climatic factors affect evapotranspiration including relative humidity, wind speed and radiation [74,75]. Compared with the baseline period, the wind speed increased by 4% in Period 2 and declined by about 3% and 23% in Period 3 and Period 4, respectively. Therefore, the actual evapotranspiration could be a little higher than the calculated in Period 2 and lower in the other two periods. Duan et al. [33], Chang et al. [76] showed that climate change and deforestation caused the melting of permafrost in the study area, which likely leads to an increase in streamflow.

## 6. Conclusions

We quantitatively evaluated the impacts of forest structure change and species composition shift on streamflow in the Tahe River watershed in northeastern China using multiple statistical models. The forest composition in the watershed gradually changed over time with young larch forests and secondary birch forests replacing old-growth larch.

We conclude that deforestation increased annual streamflow while reforestation/regrowth decreased annual streamflow. A shift in tree species composition also contributed to the reduction



of mean annual streamflow. The primitive forest ecosystem had the ability to maintain streamflow stability and reduced the risk of floods. Deforestation and the species composition shift increased the magnitude of high flow and low flow, while reforestation had the opposite result. The streamflow regimes were affected by forest structure (stock volume) and species composition.

Our results suggest that although total forest stock recovered by 2013, the flow regime did not return to the state prior to large-scale logging in the 1980s. Water yield remains higher than in the 1970s when the old-growth forest was still intact. However, it is likely that water yield in the Tahe River watershed may decrease in response to a combination of global warming and forest recovery/tree species change in the near future if precipitation does not increase. It becomes more challenging to optimize ecosystem services such as water supply and carbon sequestration through forest management practices in the study region.

**Supplementary Materials:** The following materials are available online at <http://www.mdpi.com/1999-4907/10/3/211/s1>, Text S1: Hamon method used to calculate the potential evapotranspiration ( $ET_0$ ), Table S1: The change in streamflow for the different periods when using the eight sensitivity-based approaches, Table S2: Correlation analysis of hydrological variables (high and low flow) and climatic variables, Table S3: The selected pairs for high flow, Table S4: The selected pairs for low flow, Figure S1: Changes in streamflow depth during the three periods due to forest structure and climate change estimated by the eight approaches, Figures S2–S4 show the high flow for the selected paired years in FDCs and PDCs, Figures S5–S7 show the low flow for the selected paired years in FDCs and PDCs.

**Author Contributions:** Z.Y., G.S., L.D. and T.C. conceived and designed the research experiments; Z.Y. and G.S. wrote the paper with contributions from D.W.H.; Z.Y. analyzed the data; L.D. and T.C. contributed to data collection. All authors contributed to the revision and approved the manuscript.

**Funding:** This work was financially supported by the National Natural Key R&D Program of China (2018YFC0507302) and the National Science Foundation of China (Grant No. 31770488).

**Acknowledgments:** We acknowledge the financial support from the National Key R&D Program of China (2018YFC0507302) and the National Natural Science Foundation of China (Grant No. 31770488). This work is also supported by CFERN & BEIJING TECHNO SOLUTIONS Award Funds for excellent academic achievements. Support was also provided by the China Scholarship Council for Zhengxiang Yu to visit the USDA Forest Service Southern Research Station.

**Conflicts of Interest:** The authors declare no conflict of interest.

## References

1. Zhang, M.; Liu, N.; Harper, R.; Li, Q.; Liu, K.; Wei, X.; Ning, D.; Hou, Y.; Liu, S. A global review on hydrological responses to forest change across multiple spatial scales: Importance of scale, climate, forest type and hydrological regime. *J. Hydrol.* **2017**, *546*, 44–59. [[CrossRef](#)]
2. Li, Q.; Wei, X.; Zhang, M.; Liu, W.; Fan, H.; Zhou, G.; Giles-Hansen, K.; Liu, S.; Wang, Y. Forest cover change and water yield in large forested watersheds: A global synthetic assessment. *Ecohydrology* **2017**, *10*, e1838. [[CrossRef](#)]
3. Brown, A.E.; Zhang, L.; McMahon, T.A.; Western, A.W.; Vertessy, R.A. A review of paired catchment studies for determining changes in water yield resulting from alterations in vegetation. *J. Hydrol.* **2005**, *310*, 28–61. [[CrossRef](#)]
4. Swank, W.T.; Miner, N. Conversion of hardwood-covered watersheds to white pine reduces water yield. *Water Resour. Res.* **1968**, *4*, 947–954. [[CrossRef](#)]
5. Swank, W.T.; Douglass, J.E. Streamflow greatly reduced by converting deciduous hardwood stands to pine. *Science* **1974**, *185*, 857–859. [[CrossRef](#)] [[PubMed](#)]
6. Serengil, Y.; Swank, W.T.; Riedel, M.S.; Vose, J.M. Conversion to pine: Changes in timing and magnitude of high and low flows. *Scand. J. For. Res.* **2011**, *26*, 568–575. [[CrossRef](#)]
7. Brantley, S.; Ford, C.R.; Vose, J.M. Future species composition will affect forest water use after loss of eastern hemlock from southern Appalachian forests. *Ecol. Appl.* **2013**, *23*, 777–790. [[CrossRef](#)] [[PubMed](#)]
8. Caldwell, P.V.; Miniati, C.F.; Elliott, K.J.; Swank, W.T.; Brantley, S.T.; Laseter, S.H. Declining water yield from forested mountain watersheds in response to climate change and forest mesophication. *Glob. Chang. Biol.* **2016**, *22*, 2997–3012. [[CrossRef](#)] [[PubMed](#)]



9. Elliott, K.J.; Caldwell, P.V.; Brantley, S.T.; Miniati, C.F.; Vose, J.M.; Swank, W.T. Water yield following forest–grass–forest transitions. *Hydrol. Earth Syst. Sci.* **2017**, *21*, 981–997. [[CrossRef](#)]
10. Komatsu, H.; Tanaka, N.; Kume, T. Do coniferous forests evaporate more water than broad-leaved forests in Japan? *J. Hydrol.* **2007**, *336*, 361–375. [[CrossRef](#)]
11. Komatsu, H.; Kume, T.; Otsuki, K. Increasing annual runoff—broadleaf or coniferous forests? *Hydrol. Process.* **2011**, *25*, 302–318. [[CrossRef](#)]
12. Komatsu, H.; Kume, T.; Otsuki, K. Changes in low flow with the conversion of a coniferous plantation to a broad-leaved forest in a summer precipitation region, Japan. *Ecohydrol. Ecosyst. Land Water Process Interact. Ecohydrogeomorphol.* **2009**, *2*, 164–172. [[CrossRef](#)]
13. Sun, G.; Zuo, C.; Liu, S.; Liu, M.; McNulty, S.G.; Vose, J.M. Watershed Evapotranspiration Increased due to Changes in Vegetation Composition and Structure Under a Subtropical Climate 1. *JAWRA J. Am. Water Resour. Assoc.* **2008**, *44*, 1164–1175. [[CrossRef](#)]
14. Gerrits, A.; Pfister, L.; Savenije, H. Spatial and temporal variability of canopy and forest floor interception in a beech forest. *Hydrol. Process.* **2010**, *24*, 3011–3025. [[CrossRef](#)]
15. Sun, J.; Yu, X.; Wang, H.; Jia, G.; Zhao, Y.; Tu, Z.; Deng, W.; Jia, J.; Chen, J. Effects of forest structure on hydrological processes in China. *J. Hydrol.* **2018**, *561*, 187–199. [[CrossRef](#)]
16. Wullschlegel, S.D.; Meinzer, F.; Vertessy, R. A review of whole-plant water use studies in tree. *Tree Physiol.* **1998**, *18*, 499–512. [[CrossRef](#)] [[PubMed](#)]
17. Benyon, R.; Doody, T. Comparison of interception, forest floor evaporation and transpiration in *Pinus radiata* and *Eucalyptus globulus* plantations. *Hydrol. Process.* **2015**, *29*, 1173–1187. [[CrossRef](#)]
18. Wullschlegel, S.D.; Hanson, P.; Todd, D. Transpiration from a multi-species deciduous forest as estimated by xylem sap flow techniques. *For. Ecol. Manag.* **2001**, *143*, 205–213. [[CrossRef](#)]
19. Ford, C.R.; Hubbard, R.M.; Vose, J.M. Quantifying structural and physiological controls on variation in canopy transpiration among planted pine and hardwood species in the southern Appalachians. *Ecohydrology* **2011**, *4*, 183–195. [[CrossRef](#)]
20. Sun, G.; Hallema, D.; Asbjornsen, H. Ecohydrological processes and ecosystem services in the Anthropocene: A review. *Ecol. Process.* **2017**, *6*, 35. [[CrossRef](#)]
21. Li, Q.; Wei, X.; Zhang, M.; Liu, W.; Giles-Hansen, K.; Wang, Y. The cumulative effects of forest disturbance and climate variability on streamflow components in a large forest-dominated watershed. *J. Hydrol.* **2018**, *557*, 448–459. [[CrossRef](#)]
22. Wei, X.; Zhang, M. Quantifying streamflow change caused by forest disturbance at a large spatial scale: A single watershed study. *Water Resour. Res.* **2010**, *46*, W12525. [[CrossRef](#)]
23. Wei, X.; Liu, W.; Zhou, P. Quantifying the relative contributions of forest change and climatic variability to hydrology in large watersheds: A critical review of research methods. *Water* **2013**, *5*, 728–746. [[CrossRef](#)]
24. Zhou, G.; Wei, X.; Luo, Y.; Zhang, M.; Li, Y.; Qiao, Y.; Liu, H.; Wang, C. Forest recovery and river discharge at the regional scale of Guangdong Province, China. *Water Resour. Res.* **2010**, *46*. [[CrossRef](#)]
25. Zhao, F.; Zhang, L.; Xu, Z.; Scott, D.F. Evaluation of methods for estimating the effects of vegetation change and climate variability on streamflow. *Water Resour. Res.* **2010**, *46*. [[CrossRef](#)]
26. Koster, R.D.; Suarez, M.J. A simple framework for examining the interannual variability of land surface moisture fluxes. *J. Clim.* **1999**, *12*, 1911–1917. [[CrossRef](#)]
27. Liu, Q.; Yang, Z.; Cui, B.; Sun, T. Temporal trends of hydro-climatic variables and runoff response to climatic variability and vegetation changes in the Yiluo River basin, China. *Hydrol. Process. Int. J.* **2009**, *23*, 3030–3039. [[CrossRef](#)]
28. Li, H.; Zhang, Y.; Vaze, J.; Wang, B. Separating effects of vegetation change and climate variability using hydrological modelling and sensitivity-based approaches. *J. Hydrol.* **2012**, *420*, 403–418. [[CrossRef](#)]
29. Zheng, H.; Zhang, L.; Zhu, R.; Liu, C.; Sato, Y.; Fukushima, Y. Responses of streamflow to climate and land surface change in the headwaters of the Yellow River Basin. *Water Resour. Res.* **2009**, *45*. [[CrossRef](#)]
30. Chen, H.; Zhang, W.; Gao, H.; Nie, N. Climate change and anthropogenic impacts on wetland and agriculture in the Songnen and Sanjiang Plain, northeast China. *Remote Sens.* **2018**, *10*, 356. [[CrossRef](#)]
31. An, S.; Li, H.; Guan, B.; Zhou, C.; Wang, Z.; Deng, Z.; Zhi, Y.; Liu, Y.; Xu, C.; Fang, S. China's natural wetlands: Past problems, current status, and future challenges. *AMBIO J. Hum. Environ.* **2007**, *36*, 335–342. [[CrossRef](#)]
32. Piao, S.; Ciais, P.; Huang, Y.; Shen, Z.; Peng, S.; Li, J.; Zhou, L.; Liu, H.; Ma, Y.; Ding, Y. The impacts of climate change on water resources and agriculture in China. *Nature* **2010**, *467*, 43. [[CrossRef](#)] [[PubMed](#)]

33. Duan, L.; Man, X.; Kurylyk, B.L.; Cai, T.; Li, Q. Distinguishing streamflow trends caused by changes in climate, forest cover, and permafrost in a large watershed in northeastern China. *Hydrol. Process.* **2017**, *31*, 1938–1951. [[CrossRef](#)]
34. Sun, G.; Jin, H.; Chang, X.; Yu, S.; He, R.; Yang, S.; Lu, L.; Yao, Y.; Yan, X.; Fan, Y. Effect of broad valley landform on formation of marshes in northern Da Hinggan Mountains. *J. Glaciol. Geocryol.* **2011**, *33*, 991–998.
35. Liu, J.; Kuang, W.; Zhang, Z.; Xu, X.; Qin, Y.; Ning, J.; Zhou, W.; Zhang, S.; Li, R.; Yan, C. Spatiotemporal characteristics, patterns, and causes of land-use changes in China since the late 1980s. *J. Geogr. Sci.* **2014**, *24*, 195–210. [[CrossRef](#)]
36. Poff, N.L.; Allan, J.D.; Bain, M.B.; Karr, J.R.; Prestegard, K.L.; Richter, B.D.; Sparks, R.E.; Stromberg, J.C. The natural flow regime. *BioScience* **1997**, *47*, 769–784. [[CrossRef](#)]
37. Foster, H.A. Duration curves. In *Proceedings of the American Society of Civil Engineers*; American Society of Civil Engineers: New York, NY, USA, 1934; pp. 1223–1246.
38. Vogel, R.M.; Fennessey, N.M. Flow-duration curves. I: New interpretation and confidence intervals. *J. Water Resour. Plan. Manag.* **1994**, *120*, 485–504. [[CrossRef](#)]
39. Duan, L.; Cai, T. Changes in magnitude and timing of high flows in large rain-dominated watersheds in the cold region of north-eastern China. *Water* **2018**, *10*, 1658. [[CrossRef](#)]
40. Liu, W.; Wei, X.; Fan, H.; Guo, X.; Liu, Y.; Zhang, M.; Li, Q. Response of flow regimes to deforestation and reforestation in a rain-dominated large watershed of subtropical China. *Hydrol. Process.* **2015**, *29*, 5003–5015. [[CrossRef](#)]
41. Tokarczyk, T. Classification of low flow and hydrological drought for a river basin. *Acta Geophys.* **2013**, *61*, 404–421. [[CrossRef](#)]
42. Zhang, M.; Wei, X. Alteration of flow regimes caused by large-scale forest disturbance: A case study from a large watershed in the interior of British Columbia, Canada. *Ecolhydrology* **2014**, *7*, 544–556. [[CrossRef](#)]
43. Li, L.J.; Zhang, L.; Wang, H.; Wang, J.; Yang, J.W.; Jiang, D.J.; Li, J.Y.; Qin, D.Y. Assessing the impact of climate variability and human activities on streamflow from the Wuding River basin in China. *Hydrol. Process. Int. J.* **2007**, *21*, 3485–3491. [[CrossRef](#)]
44. Hallema, D.W.; Ge, S.; Caldwell, P.V.; Norman, S.P.; Cohen, E.C.; Liu, Y.; Ward, E.J.; McNulty, S.G. Assessment of wildland fire impacts on watershed annual water yield: Analytical framework and case studies in the United States: Wildland fire impacts on annual water yield: Framework and case studies. *Ecolhydrology* **2016**, *10*. [[CrossRef](#)]
45. Shaake, J. *From Climate to Flow*, in *Climate Change and US Water Resources*; Waggoner, P.E., Ed.; John Wiley: New York, NY, USA, 1990; pp. 177–206.
46. Jones, R.N.; Chiew, F.H.; Boughton, W.C.; Zhang, L. Estimating the sensitivity of mean annual runoff to climate change using selected hydrological models. *Adv. Water Resour.* **2006**, *29*, 1419–1429. [[CrossRef](#)]
47. Sankarasubramanian, A.; Vogel, R.M.; Limbrunner, J.F. Climate elasticity of streamflow in the United States. *Water Resour. Res.* **2001**, *37*, 1771–1781. [[CrossRef](#)]
48. Chiew, F.H. Estimation of rainfall elasticity of streamflow in Australia. *Hydrol. Sci. J.* **2006**, *51*, 613–625. [[CrossRef](#)]
49. Ma, H.; Yang, D.; Tan, S.K.; Gao, B.; Hu, Q. Impact of climate variability and human activity on streamflow decrease in the Miyun Reservoir catchment. *J. Hydrol.* **2010**, *389*, 317–324. [[CrossRef](#)]
50. Budyko, M. *Evaporation under Natural Conditions*; Translated from Russian by Isr; Israel Program for Scientific Translations: Jerusalem, Israel, 1948.
51. Schreiber, P. Über die Beziehungen zwischen dem Niederschlag und der Wasserführung der Flüsse in Mitteleuropa. *Z. Meteorol.* **1904**, *21*, 441–452.
52. Ol'Dekop, E. On evaporation from the surface of river basins. *Trans. Meteorol. Obs.* **1911**, *4*, 200.
53. Pike, J. The estimation of annual run-off from meteorological data in a tropical climate. *J. Hydrol.* **1964**, *2*, 116–123. [[CrossRef](#)]
54. Fu, B. On the calculation of the evaporation from land surface. *Sci. Atmos. Sin* **1981**, *5*, 23–31.
55. Dung, B.X.; Gomi, T.; Miyata, S.; Sidle, R.C. Peak flow responses and recession flow characteristics after thinning of Japanese cypress forest in a headwater catchment. *Hydrol. Res. Lett.* **2012**, *6*, 35–40. [[CrossRef](#)]
56. Wang, S.; Fu, B.-J.; He, C.-S.; Sun, G.; Gao, G.-Y. A comparative analysis of forest cover and catchment water yield relationships in northern China. *For. Ecol. Manag.* **2011**, *262*, 1189–1198. [[CrossRef](#)]
57. Sun, G.; Caldwell, P.; Noormets, A.; McNulty, S.G.; Cohen, E.; Moore Myers, J.; Domec, J.C.; Treasure, E.; Mu, Q.; Xiao, J. Upscaling key ecosystem functions across the conterminous United States by a water-centric ecosystem model. *J. Geophys. Res. Biogeosci.* **2011**, *116*. [[CrossRef](#)]

58. Tian, Y.; Man, X.; Liu, X.; Li, Y. Research on rainfall redistribution of *Betula platyphylla* secondary forests in north of Da Hinggan Mountains. *J. Soil Water Conserv.* **2014**, *3*, 119–123.
59. Sheng, H.; Cai, T.; Li, Y. Rainfall redistribution in *Larix gmelinii* forest on northern of Daxing'an Mountains, Northeast of China. *J. Soil Water Conserv.* **2014**, *28*, 101–105.
60. Yu, Z.; Cai, T.; Zhu, B. Characteristics of snowpack in major forest types of northern Daxing'anling Mountains, northeastern China. *J. Beijing For. Univ.* **2015**, *12*, 013.
61. Ford, C.R.; Laseter, S.H.; Swank, W.T.; Vose, J.M. Can forest management be used to sustain water-based ecosystem services in the face of climate change? *Ecol. Appl.* **2011**, *21*, 2049–2067. [[CrossRef](#)] [[PubMed](#)]
62. Zhang, Y.; Wang, C. Transpiration of boreal and temperate forests. *Chin. J. Appl. Environ. Biol.* **2008**, *6*, 838–845.
63. Mu, T. The estimation of transpiration of main tree species and water consumption of larch in Da Hinggan Mountains. *Inn. Mong. For. Sci. Technol.* **1980**, *2*, 3.
64. Hümann, M.; Schüller, G.; Müller, C.; Schneider, R.; Johst, M.; Caspari, T. Identification of runoff processes—The impact of different forest types and soil properties on runoff formation and floods. *J. Hydrol.* **2011**, *409*, 637–649. [[CrossRef](#)]
65. Gebrehiwot, S.G.; Taye, A.; Bishop, K. Forest cover and stream flow in a headwater of the Blue Nile: Complementing observational data analysis with community perception. *Ambio* **2010**, *39*, 284–294. [[CrossRef](#)] [[PubMed](#)]
66. Kelly, C.N.; McGuire, K.J.; Miniati, C.F.; Vose, J.M. Streamflow response to increasing precipitation extremes altered by forest management. *Geophys. Res. Lett.* **2016**, *43*, 3727–3736. [[CrossRef](#)]
67. Cheng, J.; Black, T.; De Vries, J.; Willington, R.; Goodell, B. Evaluation of initial changes in peak streamflow following logging of a watershed on the West coast of Canada. In Proceedings of the International Symposium on Hydrological Characteristics River Basins Effects Characteristics Better Water Manage, Tokyo, Japan, 1–8 December 1975.
68. Storck, P.; Bowling, L.; Wetherbee, P.; Lettenmaier, D. Application of a GIS-based distributed hydrology model for prediction of forest harvest effects on peak stream flow in the Pacific Northwest. *Hydrol. Process.* **1998**, *12*, 889–904. [[CrossRef](#)]
69. Wu, J.; Kong, L.; Wang, J.; Lin, W. Study on hydrological characteristics of forest litters in conifer and broad-leaved mixed forests at different forest successional stages in Jiaohe, Jilin Province. *J. Nanjing For. Univ. (Nat. Sci. Ed.)* **2016**, *40*, 113–120.
70. Zhang, M.; Wei, X.; Sun, P.; Liu, S. The effect of forest harvesting and climatic variability on runoff in a large watershed: The case study in the Upper Minjiang River of Yangtze River basin. *J. Hydrol.* **2012**, *464*, 1–11. [[CrossRef](#)]
71. Eisenbies, M.; Aust, W.; Burger, J.; Adams, M.B. Forest operations, extreme flooding events, and considerations for hydrologic modeling in the Appalachians—A review. *For. Ecol. Manag.* **2007**, *242*, 77–98. [[CrossRef](#)]
72. Duan, L.L.; Man, X.L.; Kurylyk, B.L.; Cai, T.J. Increasing Winter Baseflow in Response to Permafrost Thaw and Precipitation Regime Shifts in Northeastern China. *Water* **2017**, *9*, 25. [[CrossRef](#)]
73. Duan, L.; Cai, T.J. Quantifying Impacts of Forest Recovery on Water Yield in Two Large Watersheds in the Cold Region of Northeast China. *Forests* **2018**, *9*, 392. [[CrossRef](#)]
74. Valipour, M. Analysis of potential evapotranspiration using limited weather data. *Appl. Water Sci.* **2017**, *7*, 187–197. [[CrossRef](#)]
75. Valipour, M.; Sefidkouhi, M.A.G. Temporal analysis of reference evapotranspiration to detect variation factors. *Int. J. Glob. Warm.* **2018**, *14*, 385–401. [[CrossRef](#)]
76. Chang, X.; Jin, H.; Zhang, Y.; He, R.; Luo, D.; Wang, Y.; Lv, L.; Zhang, Q. Thermal impacts of boreal forest vegetation on active layer and permafrost soils in northern Da Xing'anling (Hinggan) Mountains, Northeast China. *Arct. Antarct. Alpine Res.* **2015**, *47*, 267–279. [[CrossRef](#)]

